Ollscoil na Gaillimhe
University of Galway

Provided by the author(s) and University of Galway in accordance with publisher policies. Please cite the published version when available.

Title	Models of flow-induced loading on blood cells in laminar and turbulent flow, with application to cardiovascular device flow
Author(s)	Quinlan, Nathan J.; Dooley, Patrick N.
Publication Date	2007-08
Publication Information	Quinlan, N., & Dooley, P. (2007). Models of Flow-Induced Loading on Blood Cells in Laminar and Turbulent Flow, with Application to Cardiovascular Device Flow. "Annals of Biomedical Engineering", Vol 35(No. 8), pp 1347-1356.
Publisher	Springer
Link to publisher's version	http://dx.doi.org/10.1007/s10439-007-9308-8
Item record	http://hdl.handle.net/10379/313

Downloaded 2024-04-17T21:21:40Z

Some rights reserved. For more information, please see the item record link above.

Ann. Biomed. Eng. manuscript No.
(will be inserted by the editor)

Models of flow-induced loading on blood cells in laminar and turbulent flow, with application to cardiovascular device flow

Nathan J. Quinlan, Patrick N. Dooley

National Centre for Biomedical Engineering Science and Department of Mechanical and Biomedical Engineering, National University of Ireland, Galway, Ireland
e-mail: nathan.quinlan@nuigalway.ie

Received: date / Revised version: date

Abstract Viscous shear stress and Reynolds stress are often used to predict hemolysis and thrombosis due to flow-induced stress on blood elements in cardiovascular devices. These macroscopic stresses are distinct from the true stress on an individual cell, which is determined by the local microscale flow field. In this paper the flow-induced stress on blood cells is calculated for laminar and turbulent flow, using simplified models for cells and for turbulent eddies. The model is applied to estimate shear stress on red blood cells in flow through a prosthetic heart valve, using the energy spectral density measured by Liu et al. (*J. Biomech.* 34:1361–1364, 2000). Results show that in laminar flow, the maximum stress on a cell is approximately equal to

the macroscopic viscous shear stress. In turbulent flow through a prosthetic heart valve, the estimated root mean square of flow-induced stress on a cell is at least an order of magnitude less than the Reynolds stress. The results support the hypothesis that smaller turbulent eddies cause higher stress on cells. However, the stress due to an eddy depends on the velocity scale of the eddy as well as its length scale. For the heart valve flow investigated, turbulence contributes to flow-induced stress on cells almost equally across a broad range of the frequency spectrum. The model suggests that Reynolds stress alone is not an adequate predictor of cell damage in turbulent flow, and highlights the importance of the energy spectral density.

Key words turbulent blood flow – laminar blood flow – prosthetic heart valves – hemolysis – Reynolds stress – energy spectral density

1 Introduction

In the development of cardiovascular implants such as mechanical heart valves[7,12,37] and ventricular assist devices[2,6], it is desirable to predict the occurrence of mechanically induced thrombosis and hemolysis as a function of flow field parameters. Usually, such blood damage is predicted as functions of viscous shear stress (for laminar flow) or Reynolds stress (for turbulent flow), on the basis of *in vitro* experiments on blood. These parameters describe blood flow at a macroscopic level. However, it is at the cellular scale that thrombosis and hemolysis are initiated, and the viscous

stress and Reynolds stress do not directly describe the microscopic flow field experienced by red blood cells and platelets.

The purpose of this paper is to estimate the flow-induced loading on individual blood cells as a function of macroscopic flow parameters which can be measured *in vitro*. Approximate analytical models will be presented in which shear stress on the cell surface is calculated as a function of macroscopic viscous and Reynolds stresses for laminar and turbulent flows, respectively. Quantitatively accurate results are not expected from these models; the objective is to explore the relationship between measurable macroscopic stresses and the true stress on blood cells in order-of-magnitude terms.

Attention is restricted to hemolysis in this paper, but the arguments are equally applicable to thrombosis or any biological or biomechanical response to mechanical loading of suspended blood elements. Table 1 and Table 2 give a summary of previously published values of viscous shear stress and Reynolds shear stress thresholds above which significant hemolysis occurs in laminar and turbulent flow, respectively. For turbulent flow, the Reynolds stress threshold of 400 Pa reported by Sallam and Hwang[28] is widely accepted. Lu et al.[21] conducted new measurements of the flow field used by Sallam and Hwang to expose blood cells to turbulent flow, and suggested that the threshold should be revised upwards to 800 Pa.

It is important to note that Reynolds stress and viscous stress have fundamentally different meanings. The viscous shear stress is $\sigma_{v,ij} = \mu \partial u_i / \partial x_j$ in a Newtonian fluid, where u_i denotes a velocity component in coordinate

Table 1 Minimum viscous stress σ_v and corresponding estimated exposure time t_{exp} for onset of hemolysis in laminar flow.

Source	t_{exp}(s)	σ_v(Pa)
Bacher and Williams[1]	0.107–0.321	500
Hellums and Brown[14]	120	150
Heuser and Opitz[15]	0.05	450
Leverett et al.[19]	120	150
Nevaril et al.[23]	120	300
Paul et al.[26]	0.62	425
Rooney[27]	10^{-3}	450±150
Williams et al.[33]	10^{-4}	560
Wurzinger et al.[35]	0.056-0.113	150

Table 2 Minimum Reynolds shear stress σ_R and corresponding estimated exposure time t_{exp} for onset of hemolysis in turbulent flow.

Source	t_{exp}(s)	σ_R(Pa)
Blackshear et al.[3]	–	3000
Forstrom[9]	10^{-5}	5000
Sallam and Hwang[28]	10^{-3}	400
Sutera and Mehrjardi[30]	240	2500

direction x_i, and μ is the fluid's dynamic viscosity. The concept of Reynolds stress arises when the Navier-Stokes equations are averaged over time scales longer than the time scales of turbulent fluctuations (or averaged over a large ensemble of experiments). The resulting equations include terms of the form $\rho\overline{u_i' u_j'}$, where ρ is the fluid density, u_i' and u_j' denote turbulent velocity fluc-

tuations about the mean, and the overbar denotes the average. These terms represent the time- or ensemble-averaged momentum flux associated with turbulent fluctuations (see, for example, Bradshaw[4], Davidson[5]). When the average flow is analysed, these momentum fluxes can be interpreted as apparent stresses – the Reynolds stresses $\sigma_{R,ij}$ – which are required to satisfy conservation of momentum. Both laminar and turbulent flow are governed by the Navier-Stokes equations, and at sufficiently short length and time scales, there is no fundamental difference. It is only at macroscopic scales that the unsteady, three-dimensional, chaotic nature of turbulence is apparent, and statistical descriptions such as the Reynolds stress are then valuable.

Kameneva et al.[17] showed definitively that laminar and turbulent blood flows have quantifiably different hemolytic effects. By suspending red blood cells at hematocrit of 24% in solutions of varying viscosity, they generated laminar and turbulent pipe flows of equal mean wall viscous shear stress. Hemoglobin release in the turbulent flow exceeded that in the laminar flow by a factor of 6, confirming that turbulent fluctuations cause damage which cannot be attributed to the underlying mean shear flow.

Giersiepen et al.[11] analysed the laminar flow hemolysis data of Wurzinger et al.[35], and developed a simple and useful equation for prediction of hemolysis as a function of viscous shear stress and exposure time. However, the subsequent use of this equation to predict hemolysis in turbulent flow is flawed, as it implies an equivalence between viscous and Reynolds stress.

Grigioni et al.[13] treated the Reynolds stress as a quantitative estimate of true shear stress on the cell membrane. However, there is a complex local flow of plasma around every cell, which determines the stress distribution on the surface of the cell. In a turbulent flow, the largest eddies simply transport a cell with low acceleration and low stress. A cell in a small eddy may be exposed to high velocity gradients and rapid velocity changes in its local flow field. Reynolds stress cannot be equal to the true stress on the cell, since it does not discriminate between the effects of different length scales. In fact, the Reynolds stress at the cell membrane is always zero (in the reference frame of the cell membrane) because normal and tangential fluid velocity relative to a solid boundary must equal zero, as pointed out by Sutera and Joist[29]. Thus, there is a need for clarity as to the physical meaning of both viscous and Reynolds stresses at the cellular scale, and their influence on loading of individual cells.

Jones[16] developed an estimate of local viscous stress in turbulent flow based on an energy balance for homogeneous, statistically stationary, turbulence, and argued that this stress is more meaningful than Reynolds stress for prediction of blood damage. However, the proposed stress parameter is derived for a homogeneous fluid, without consideration of the direct loading of cells by the local microscale plasma flow. In an analysis of the data of Sallam and Hwang[28], Jones showed that this viscous stress parameter is an order of magnitude lower than the Reynolds stress.

It has been suggested[7,21] that turbulent flow can damage blood cells only if the size of the smallest eddies (estimated by the Kolmogorov length scale, η) is comparable to cell size. However, there is no direct experimental evidence that this is the case. Reliance on Reynolds stress as the sole predictor of blood damage is incompatible with this hypothesis, as length scales are not uniquely determined by Reynolds stress. Turbulent flow has not been measured directly at the scale of blood cells and the smallest eddies, but the Kolmogorov length scale has been calculated from macroscopic experimental data by some researchers. For mechanical prosthetic heart valve flows, the Kolmogorov scale has been reported by Ellis et al.[7] as 7 μm in the hinge flow, by Liu et al.[20] as 25–47 μm in forward flow, and by Travis et al.[32] as 36–72 μm for leakage jets *in vivo*. However, the assumptions underlying Kolmogorov theory (homogeneous, isotropic, statistically stationary turbulence) may not be applicable in the short-duration peak flow through a heart valve.

An effective methodology for prediction of blood damage in design of medical devices should account for the microscale flow field, which determines the true stress on cells. This local flow around a cell is determined in turn by the macroscopic flow field, which can be measured *in vitro* or perhaps computed. Neither Reynolds stress nor Jones' viscous stress parameter are entirely satisfactory as the sole predictor of blood damage in turbulent flow, since they are not sensitive to the distribution of energy across the spectrum from microscopic to macroscopic length scales. In this paper, a

simplified model is developed for the microscale flow, and the resulting flow-induced shear stress on cells is estimated in a new theoretical framework which incorporates the effect of turbulent length scales. This approach allows the shear stress on cells to be estimated from experimental data for turbulent blood flow, as shown in an example. This framework is expected to yield results for shear stress on the cell membrane which are accurate to better than an order of magnitude, in order to develop quantitative insight and to compare the effects of different flow conditions.

2 Analysis for laminar flow

A red blood cell (RBC) consists of a flexible but nearly inextensible membrane containing liquid cytoplasm[10]. In the absence of external loads, the membrane relaxes to a biconcave disc of typical diameter 8 μm and maximum thickness 2.6 μm. However, under steady laminar shear flow, RBCs assume an ellipsoidal shape due to the tank-treading phenomenon[8]. Sutera and Mehrjardi[30] found that cells were elongated and ellipsoidal in shape after fixing with glutaraldehyde in turbulent flow. However, the deformed shape of cells in turbulent flow has never been observed directly. In the present work, the red blood cell is approximated as an isolated rigid sphere of diameter 8 μm. This approximation is expected to have a minor effect on the values of flow-induced stress, as the the key mechanics of plasma flow around the cell are represented at the correct scales. The objective to obtain

order-of-magnitude estimates is not compromised by the simplification of cell shape and structure.

The red blood cell is modelled as a sphere of diameter $2a = 8$ μm and density 1100 kg/m^3. Plasma is taken as incompressible and Newtonian, with dynamic viscosity $\mu = 1.2$ mPas and density $\rho = 1030$ kg/m^3. These are representative mechanical properties given by Fung[10].

The flow of plasma is governed by the Navier-Stokes equations, as follows:

$$\rho \frac{\partial u_i}{\partial t} + \rho u_j \frac{\partial u_i}{\partial x_j} = -\frac{\partial p}{\partial x_i} + \mu \frac{\partial^2 u_i}{\partial x_j \partial x_j} \ , \tag{1}$$

where u is a velocity component, indices i and j denote coordinate directions, and summation over repeated indices is implied. In principle, the shear stress on the cell surface can be determined from the velocity field obtained by solution of the governing equations. General shear stresses in spherical coordinates are given by Landau and Lifshitz[18] as follows:

$$\begin{aligned} \sigma_{r\phi} &= \mu \left(\frac{1}{r} \frac{\partial u_r}{\partial \phi} + \frac{\partial u_\phi}{\partial r} - \frac{u_\phi}{r} \right) \\ \sigma_{r\theta} &= \mu \left(\frac{\partial u_\theta}{\partial r} + \frac{1}{r \sin \phi} \frac{\partial u_r}{\partial \theta} - \frac{u_\theta}{r} \right) \ , \end{aligned} \tag{2}$$

where θ and ϕ are the azimuthal and polar angles, respectively. Shear stress on the cell surface is calculated by evaluating Eq. (2) at $r = a$, with the origin of the coordinate system located at the centre of the cell.

The Reynolds number for plasma flow relative to a blood cell, based on cell diameter, is always much less than 1. As a result, all terms in the Navier-Stokes equations are negligible in comparison with the viscous stress.

The reduced equation $\mu\,\partial^2 u_i/\partial x_j \partial x_j = 0$ is linear, so that any velocity fields which satisfy the governing equations and boundary conditions can be superimposed additively to obtain a new velocity field which is also a valid solution. The corresponding cell surface stresses also combine additively.

In a laminar physiological blood flow, unsteadiness occurs on timescales which are very long compared to the transient response of a cell to changes in the local velocity field. Therefore, it is assumed that a cell suspended in a laminar flow is in equilibrium – it experiences zero net drag and torque. The local spatial structure of the laminar flow can be described by the shear rate alone. This can be justified for an arbitrary macroscopic laminar velocity field by taking a Taylor series for velocity in the neighbourhood of a single cell. The problem then is to determine the shear stress on a spherical cell in equilibrium with a steady linear velocity profile in the surrounding fluid. Mikeluncak and Morris[22] give an exact solution for the velocity field. Application of Eq. (2) to that solution gives the stresses on the the cell surface as follows:

$$\begin{aligned} \frac{\sigma_{r\theta}}{\mu\dot{\gamma}} &= \frac{5}{2}\cos\phi\cos\theta \\ \frac{\sigma_{r\phi}}{\mu\dot{\gamma}} &= \frac{5}{2}\cos 2\phi\sin\theta. \end{aligned} \tag{3}$$

The resultant shear stress on the surface of the sphere is $\left(\sigma_{r\theta}^2 + \sigma_{r\phi}^2\right)^{1/2}$, which has a maximum value of $(5/2)\mu\dot{\gamma}$ at $\phi = 0$ and a mean of $(1.483)\mu\dot{\gamma}$. Therefore, since the apparent viscosity μ_b of whole blood at high shear is around three times the viscosity μ of plasma[10], the maximum stress on the model cell, $(5/2)\mu\dot{\gamma}$, is similar to the apparent bulk shear stress $\mu_b\dot{\gamma}$.

Fischer[8] observed that red blood cells assume a steady ellipsoidal shape in steady laminar shear flow, with the membrane rotating in a tank-treading motion. Niimi and Sugihara[24] simulated this phenomenon with a 2D numerical model incorporating the intracellular flow, and found that the peak shear stress on the cell membrane is about $4\mu\dot{\gamma}$, that is, 4 times the viscous stress based on plasma viscosity and bulk velocity gradient. Tran-Son-Tay et al.[31] developed an analytical model for flow about an ellipsoidal tank-treading red blood cell and tension in the membrane. Their model predicts maximum external shear stresses from $(3.8)\mu\dot{\gamma}$ to $6\mu\dot{\gamma}$, depending on the bulk velocity gradient. These results are broadly consistent with the result of $(5/2)\mu\dot{\gamma}$ obtained above, confirming that the simplifications adopted here yield reasonable order-of-magnitude results. For the present purposes, the simplified model is preferable to more sophisticated approaches because of its generality and flexibility, which enable application to other flow types, as shown in the next section.

3 Analysis for turbulent flow

In this section, the mathematical model is developed to investigate the effect of turbulent flow on suspended cells across a range of time and length scales. The approach is to consider an isolated cell in a turbulent eddy of idealised structure, characterised by a velocity scale and a length or frequency scale . This model can be used to represent an eddy of any size. Although the basic model is developed for a single time or length scale, the linearity

of the governing equations at low Reynolds number can be exploited to evaluate the aggregate effects of turbulent eddies across all scales. Although the Reynolds number of a macroscopic turbulent flow (for example, in a prosthetic heart valve) is high, the Reynolds number for the microscale flow relative to a cell is low. Since the smallest turbulent flow features are of the order of cell size or larger, as discussed in Section 1, there is no fundamental distinction between turbulent and laminar plasma flow at the cellular scale.

Two models of cell loading in a turbulent eddy are considered in Sections 3.1 and 3.2 below. In the first case, the relative velocity between plasma and cell is considered in a time-domain approach. Because of the cell's inertia, a velocity fluctuation of the surrounding plasma results in a relative flow between the plasma and the cell, with a resultant shear stress. This effect is modelled by assuming a plasma velocity which fluctuates in time but is uniform in space. In the second case, the instantaneous spatial structure of a turbulent eddy is considered. The spatial velocity gradient in a turbulent eddy contributes to shear stress on a cell, just as in laminar flow; in a relatively large turbulent eddy, a cell experiences quasi-steady, simple shear flow.

3.1 Velocity fluctuation effects

As a cell is swept through the flow field, it interacts with turbulent eddies and encounters fluctuating plasma velocity. In the reference frame of the cell, the apparent rate and amplitude of a plasma velocity fluctuation depend

on the velocity of the cell as well as the local plasma flow field in the eddy. Although the relative velocity between plasma and cell is zero at the cell membrane, the velocity of the cell relative to surrounding plasma is in general non-zero. This relative velocity results in a net force on the cell, causing acceleration which in turn affects the relative velocity. If a turbulent eddy in the plasma flow about the cell is significantly larger than the cell itself, then the spatial structure of the eddy is not apparent at cellular scale. Therefore, the simplified model for cell response to temporal velocity fluctuations consists of a sphere immersed in an unsteady freestream flow at a fluctuating velocity $u_\infty(t) = u_{\infty,0}\mathrm{e}^{i(2\pi f)t}$, which is uniform at large distances from the cell. A complex representation of velocity is chosen for convenience, and only the real component is considered physical. In response to the fluid velocity, the rigid, non-rotating cell is driven at velocity $v(t)$ in the flow direction. The velocities $v(t)$ and $u_\infty(t)$ are expressed in a laboratory reference frame. The choice of a sinusoidal oscillation of the freestream velocity is not restrictive, since any velocity function can be expressed as a sum or integral of sinusoidal components, and the linearity of the governing equations allows solutions for various frequencies, phases and directions to be superimposed.

Flow around the model cell is governed by Eq. (1), and as the Reynolds number is small at the scale of a cell, the viscous stress dominates. In this case, however, the pressure gradient and local acceleration terms are retained for completeness, and only the convective acceleration term is omit-

ted from the analysis. The new momentum equation is

$$\rho \frac{\partial u_i}{\partial t} = -\frac{\partial p}{\partial x_i} + \mu \frac{\partial^2 u_i}{\partial x_j \partial x_j} \ . \tag{4}$$

Landau and Lifshitz[18] give an exact solution to Eq. (4) for the special case of a sphere oscillating in still fluid. With a change of reference frame, their solution can be adapted to the present problem of an oscillating freestream flow to determine the motion of the cell and the complete flow field for the rigid, non-tank-treading, model.

The velocity $v'(t)$ of the sphere relative to the freestream flow is given by

$$v'(t) = v(t) - u_\infty(t) = v'_0 \mathrm{e}^{i(2\pi f t + \alpha)} \ , \tag{5}$$

where α is a phase angle. In the solution of Eq. (4), the amplitude v'_0 is given by

$$\frac{v'_0}{u_{\infty,0}} = \frac{2\pi f (m_p - m_c)}{\sqrt{(2\pi f)^2 \left(A(f) + m_c\right)^2 + B(f)^2}} \ , \tag{6}$$

where A and B are functions of f defined as follows.

$$\begin{aligned} A(f) &= 3\pi a^2 \sqrt{\frac{\mu\rho}{\pi f}} \left(1 + \frac{2}{9} a \sqrt{\frac{\rho \pi f}{\mu}}\right) \\ B(f) &= 6\pi\mu a \left(1 + a\sqrt{\frac{\rho\pi f}{\mu}}\right) \end{aligned} \tag{7}$$

From this solution, the shear stress on the cell surface can be determined as a function of location on the cell surface and of time. Its maximum value, in spherical coordinates, is given by

$$\sigma_{r\phi,\max} = \frac{3}{2}\mu \left[\left(\frac{1}{a} + \sqrt{\frac{\rho\pi f}{\mu}}\right)^2 + \frac{\rho\pi f}{\mu}\right]^{\frac{1}{2}} \times$$

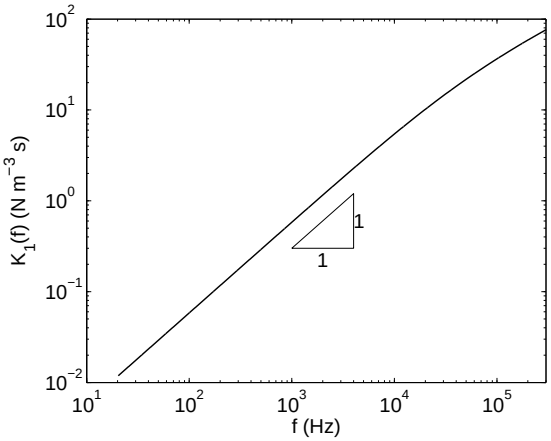

Fig. 1 The function $K_1(f)$, which is the ratio of maximum cell surface shear stress to velocity fluctuation amplitude for a plasma velocity fluctuation at frequency f.

$$\frac{2\pi f(m_p - m_c)}{\sqrt{(2\pi f)^2(A(f) + m_c)^2 + B(f)^2}}\, u_{\infty,0} = K_1(f) u_{\infty,0} \,. \tag{8}$$

where m_c is the mass of the cell and m_p is the mass of plasma displaced by the cell. The function $K_1(f)$ is defined here to describe the relationship between maximum stress and velocity fluctuation amplitude. A plot of $K_1(f)$ is shown in Fig. 1. It is nearly linear in the range of frequencies of interest.

Landau and Lifshitz[18] showed that Eq. (4) is a good approximation if $f \ll \mu/(2\pi\rho a^2)$ and $\mathrm{Re}_a = \rho v_0' a/\mu \ll 1$; in Section 4.1, these criteria will be checked in application of the analysis to a particular cardiovascular device flow field.

3.2 Analysis for velocity gradient effects

To estimate stress on a cell due to the non-uniformity of the instantaneous velocity field, a turbulent eddy of length scale L and velocity scale u_0 (relative to mean flow) is considered. The instantaneous velocity gradient $\dot{\gamma}$ in this eddy is of the order of u_0/L. The model developed in Section 2 can now be applied to estimate the shear stress as $\sigma = (5/2)\mu\dot{\gamma} = (5/2)\mu u_0/L$.

It is difficult to measure the length scale of turbulent flow structures directly. However, Taylor's frozen-field hypothesis[4,5] can be invoked to derive eddy length scale information from pointwise experimental measurements (such as data from laser Doppler velocimetry or hot-wire anemometry). Taylor's hypothesis states that if velocity fluctuations are small compared to the mean velocity, then turbulent eddies change relatively slowly as they are convected at the mean velocity $\overline{u}$. The characteristic frequency of an eddy of length scale L observed at a point in the flow is $f \simeq \overline{u}/L$. Therefore, the shear stress estimated above as a function of length scale can be expressed in terms of frequency as

$$\sigma \simeq \frac{5}{2}\mu\frac{u_0}{\overline{u}}f = K_2(f)u_0 \tag{9}$$

where $K_2(f)$ is defined as $(5\mu f)/(2\overline{u})$. Since cell inertia does not play a role in this mechanism of cell loading, $K_2(f)$ is independent of the density of the cell and plasma.

Both $K_1(f)$ and $K_2(f)$ increase with frequency, indicating that cells will experience higher stress in a small eddy than in a larger eddy of similar

velocity scale. However, this does not imply that the smallest eddies are always the most harmful to cells. To assess the potential for cell damage in a specific flow field, the relative intensity of turbulence at different length scales and frequencies must be considered. In the next section, this process is carried out for a specific example of flow through a prosthetic heart valve.

4 Application to turbulent flow downstream of a prosthetic heart valve

Liu et al.[20] reported laser Doppler velocimetry (LDV) measurements of turbulent flow downstream of prosthetic mechanical heart valves *in vitro*. The models described in Section 3 will now be used to estimate the shear stress which would be experienced by suspended cells in this flow.

4.1 Experimental turbulent energy spectra

The energy spectral density $E(f)$ of a fluctuating velocity signal $u'(t)$ is defined such that $E(f)\mathrm{d}f$ is the contribution to the mean square velocity fluctuation $\overline{u'^2}$ from fluctuations in any given frequency band. Physically, $\overline{u'^2}$ is twice the total kinetic energy per unit mass associated with velocity fluctuations. Thus, the energy spectral density $E(f)$ is a measure of the distribution of energy across frequencies. It is calculated from experimental data as the Fourier transform of the autocorrelation of $u'(t)$. Fig. 2 shows the normalised energy spectral density $E(f)/\overline{u'^2}$ measured by Liu et al.[20] for flow on the centreline 7.8 mm downstream of a St. Jude Medical bileaflet

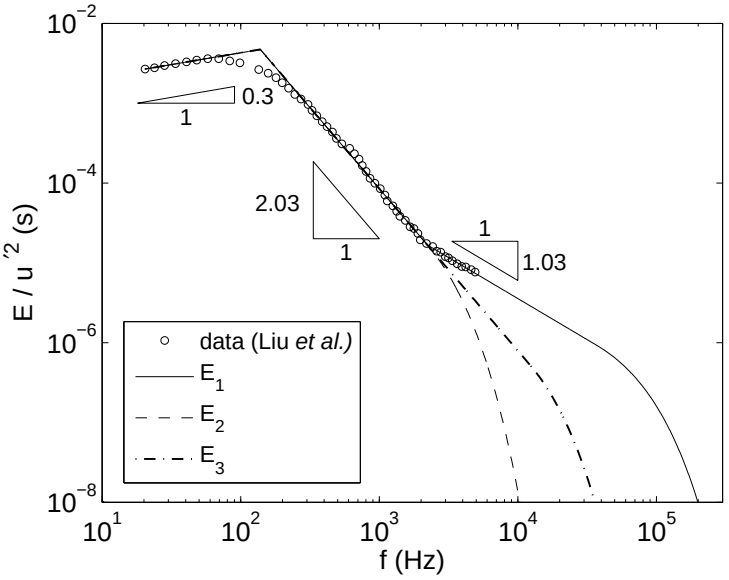

Fig. 2 Normalised energy spectral density reported by Liu et al.[20] for flow on the centreline 7.8 mm downstream of a St. Jude Medical bileaflet valve at peak flow, based on LDV measurements. The data were digitised to within 1% of the full (logarithmic) scale from a graph published by Liu et al. E_1, E_2 and E_3 are piecewise power law fits to the data, with exponential decay at high frequencies.

valve at peak flow. Also shown are a number of fits and extrapolations of the data, discussed in detail below. This spectrum is used in the present work to investigate the interaction of blood cells with turbulent flow over a full spectrum of time and length scales. The data of Liu et al.[20] can be quite accurately represented by a piecewise power law with exponents 0.30, -2.03 and -1.03.

The mean velocity $\overline{u}$ reported by Liu et al.[20] for this case is 1.69 m/s and the root mean square velocity fluctuation $(\overline{u'^2})^{1/2}$ is 0.20 m/s, giving a

turbulence intensity of 12%. The Reynolds stress $\rho\overline{u'_x u'_x}$ is 52 Pa, and the Reynolds shear stresses $\rho\overline{u'_x u'_y}$ etc. are zero at the centreline (where this particular spectrum is measured) because of symmetry of the mean flow. Liu et al.[20] calculated the Kolmogorov length scale as 46 μm.

At a turbulence intensity of 12%, the Taylor hypothesis is reasonable to within the accuracy required for this analysis. Therefore, at a mean velocity of 1.69 m/s and Kolmogorov scale of 46 μm, the smallest eddies would manifest themselves as fluctuations at a characteristic frequency of about 37 kHz. Because of instrumentation and signal processing limitations, Liu et al.[20] reported spectral data for frequencies up to 5 kHz. Therefore, extrapolation is required to carry out calculations of flow-induced stress due to fluctuations at the highest frequencies. A number of possible extrapolations are considered here, representing a range of possible scenarios.

The simplest option is to extrapolate the high-frequency segment of the power law up to 37 kHz and assume an exponential decay of energy at higher frequencies. The resulting spectrum is designated E_1 and shown in Fig. 2. However, the increase in the power-law exponent from -2.03 to -1.03 at 2 kHz, evident in the experimental data, is highly unusual for a turbulent energy spectrum. Furthermore, it is known that LDV measurements can overestimate the energy spectrum at high frequency due to the particle-rate filter effect (Nobach et al.[25] demonstrate a clear example). It is possible that the lower rate of decay at higher frequencies, observed by Liu et al.[20], is an example of this artifact. It is also possible that the Kolmogorov scale

(46 μm) is an underestimate of the size of the smallest eddies, since the assumptions underlying the calculation of this length scale may not be valid for this short-duration flow.

In light of the fact that experimental data are unavailable for frequencies above 5 kHz and may be unreliable above 2 kHz, two more spectra have been constructed. In the spectrum E_2, all data above 2 kHz are ignored. E_3 is an intermediate case between the extremes of E_1 and E_2, with the power-law exponent of -2.03 extrapolated up to 12 kHz. In all three cases, rapid exponential decay is assumed for frequencies above the upper limit of the power-law range. These assumed spectra cover a range of possible interpretations of the experimental data and allow the effects of spectral structure to be investigated.

4.2 Method

The validity of the mathematical approximations of Section 3 can now be checked for the flows represented by the spectra shown in Fig. 2. Eqs. (5) and (6) can be used to determine the amplitude v_0' of oscillations of cell velocity relative to plasma at any frequency, given the amplitude $u_{0,\infty}$ of bulk fluid velocity oscillations (which can be determined from the energy spectral density by integration over any frequency band). By integrating over the whole frequency spectrum, the root mean square velocity of a suspended cell relative to plasma, $v'_{0,rms}$, can be determined. Among the three spectra represented in Fig. 2, the highest value of $v'_{0,rms}$ is 0.0012 m/s for

$E_1(f)$, corresponding to $\mathrm{Re}_a \simeq 0.0041 \ll 1$. The parameter $\mu/(2\pi\rho a^2)$ evaluates to approximately 11600 Hz. Thus, for validity of the linear governing equations for flow about an oscillating sphere (Section 3.1), the Reynolds number criterion of Landau and Lifhsitz is satisfied, but the frequency criterion $f \ll \mu/(2\pi\rho a^2)$ is not satisfied over the whole of the spectrum E_1. Accurate solutions to Eq. (4) should not be expected for frequencies above a few kHz.

The Kolmogorov length scale of 46 μm suggests that the smallest structures in this flow are several times larger than the cell diameter. This is consistent with the simple picture of a cell suspended in an eddy and subjected to shear due to the internal velocity gradient of the eddy, which underlies the analysis of Section 3.2.

The analytical models presented in Sections 3.1 and 3.2 provide relationships of the form $\sigma_0 = K(f)u_0$ between the amplitudes of velocity and stress fluctuations. The mean square stress due to a velocity fluctuation at a discrete frequency f is therefore $\overline{\sigma^2} = (K(f))^2\,\overline{u^2}$. Since the mean square velocity in an infinitesimally narrow frequency band is $E(f)\mathrm{d}f$, the mean square stress due to velocity fluctuations in that band is $(K(f))^2\,E(f)\mathrm{d}f$. The overall mean square stress on a cell is therefore calculated by integrating $(K(f))^2\,E(f)$, which can be regarded as a spectral density for stress, as follows:

$$\overline{\sigma^2} = \int_0^\infty (K(f))^2\,E(f)\mathrm{d}f\ . \tag{10}$$

This calculation follows directly from the relationship $\sigma_0 = K(f)u_0$ and the definition of the energy spectral density $E(f)$. The validity of this calculation step does not depend on linearity of the governing equations, or any other special properties of the stress and velocity fluctuations.

4.3 Results

Calculations of $(K(f))^2 E(f)$ have been carried out for both velocity fluctuation effects using $K_1(f)$ (the model presented in Section 3.1) and velocity gradient effects using $K_2(f)$ (Section 3.2), based on three approximations to the spectral data of Liu et al. (Fig. 2). Results are shown in Fig. 3. The spectral density of stress due to velocity gradient effects is greater than that due to velocity fluctuations.

These results show that the shape of the energy spectral density is crucial in determining the effect of high frequency fluctuations (small eddies). If the energy falls off slowly with increasing frequency, as in spectrum E_1 from 2 kHz to about 70 kHz, then the stress increases with frequency. Inspection of Eq. (10) shows that an exponent of 2 in the spectrum is critical, because the stress spectrum is proportional to $(K(f))^2$, and $K(f)$ is approximately proportional to f in both models. Thus, over the large frequency ranges where the spectrum decays with an exponent of -2.03, all frequencies contribute almost equally to stress. The analysis of Section 3 shows that flow-induced stress increases with the characteristic frequency of an eddy or fluctuation, but this trend is almost exactly balanced by the decay of energy with in-

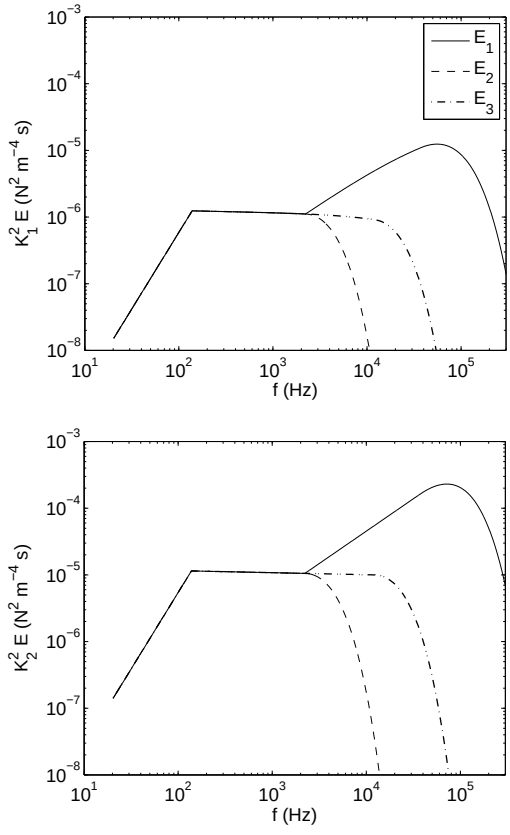

Fig. 3 Stress spectra $(K(f))^2 E(f)$ for each of the energy spectral density functions E_1, E_2 and E_3 defined in Fig. 2, for shear stress due to (a) velocity fluctuation effects ($K(f) = K_1(f)$) and (b) velocity gradient effects ($K(f) = K_2(f)$).

creasing frequency in the typical turbulent spectrum considered here. The smallest eddies in a turbulent flow are not necessarily the most damaging to cells.

The final outcome of this analysis is the root mean square stress. It has been calculated by integrating the stress spectral density according to Eq. (10), and results are tabulated in Table 3. The highest stresses are

Table 3 Estimated root mean square shear stress (Pa) on cells in turbulent flow, based on application of the present analysis to the data of Liu et al.[20], for three possible energy spectral density functions, and for velocity fluctuation effects ($K(f) = K_1(f)$) and velocity gradient effects ($K(f) = K_2(f)$).

	E_1	E_2	E_3
$\sigma_{rms,1} = \left(\int_0^\infty (K_1(f))^2 E(f)\mathrm{d}f\right)^{1/2}$ (Pa)	1.194	0.073	0.156
$\sigma_{rms,2} = \left(\int_0^\infty (K_2(f))^2 E(f)\mathrm{d}f\right)^{1/2}$ (Pa)	5.565	0.227	0.522

predicted for spectrum E_1 because of the increase in power-law exponent from -2.03 to -1.03 in the experimental spectrum of Liu et al.[20], which may be an artifact due to the particle-rate filter effect in LDV, as discussed in Section 4.1. In every case, stress due to velocity gradient effects (based on $K_2(f)$) is greater than stress due to velocity fluctuations (based on $K_1(f)$). The highest stress predicted by any of the models is less than 6 Pa and an order of magnitude less than the Reynolds stress (52 Pa). The highest stress calculated for spectra E_2 and E_3 is two orders of magnitude less than the Reynolds stress.

5 Discussion

Two major results have been presented. The first is the calculation that shear stress on a suspended cell in laminar flow is similar to the nominal bulk shear stress. The second is the set of shear stress calculations for turbulent flow summarised in Table 3, which should be regarded as order-of-magnitude estimates of flow-induced shear stress on cell surfaces due to

turbulent flow through a prosthetic heart valve. They show that the shear stress experienced by cells in turbulent flow is an order of magnitude less than the Reynolds stress, which is often taken as the primary or sole descriptor of turbulence in blood, and has sometimes been misinterpreted as an estimate of stress on the cell. These conclusions only require that the analysis is accurate to within an order of magnitude.

The uncertainty in the present analysis of turbulent flow is greatest for smallest eddies and highest frequencies, when the linearity of the governing equations breaks down, the presence of a cell in an eddy may significantly perturb its structure, and spectral experimental data are not available. At moderate frequencies up to at least 2 kHz, however, the analytical results for stress due to velocity fluctuation and cell inertia effects are expected to be reliable. Results for velocity gradient effects are expected to be reliable across the spectrum, due to the relatively large Kolmogorov length scale of the heart valve flow[20] used here as an example. However, it should be noted that Kolmogorov length scale may not be a reliable indicator of the size of the smallest eddies in the short-duration transient peak flow through a heart valve.

As shown in Fig. 3, for the turbulent flow data considered here, cell stress is independent of frequency over a broad range, and increases with frequency (or with decreasing eddy size) only in regions where the energy spectrum decays relatively slowly. This suggests that cell damage due to turbulent eddies may not be strongly dependent on eddy length scale, and

that the smallest eddies in a flow are not necessarily the most damaging. However, the analysis provides no results for eddies which are smaller than cells, or for wall effects.

According to the models developed here, stress on cells in turbulent flow is proportional to the magnitude of velocity fluctuations, since $K_1(f)$ is approximately linear and $K_2(f)$ is exactly linear. However, Reynolds stress is proportional to products of two velocity fluctuations. This leads to the interesting prediction that in turbulent flow, the shear stress on cells scales with the square root of the macroscopic Reynolds stress. If there are very small eddies and high frequencies, where the linearity of the governing equation breaks down, this relationship may not hold.

It should be emphasised that stresses calculated here are root mean square values. In turbulent flow, damage may be caused by instantaneous maxima of stress which are much higher than the root mean square values calculated here, as suggested by Jones[16]. It is also likely that fatigue damage accumulates; the well-known sensitivity of both red blood cells[35] and platelets[34,36] to exposure time suggests that these blood elements are susceptible to fatigue. Suspended cells experience fatigue loading due to turbulent fluctuations, pulsatility, and cycling through various flow regimes in the cardiovascular system. Even in steady laminar flow, a red blood cell membrane is subject to oscillating tension due to tank-treading.

It has been shown that the shear stress on a cell depends strongly on the energy spectral density of turbulence, and not just on the Reynolds stress.

This suggests that there can be no universal correlation between Reynolds stress and blood damage; for example, heart valve flow fields with the same values of Reynolds stress might have quite different spectra, resulting in different values of stress on cells.

This approximate analysis shows that it is possible, in principle, to estimate the flow-induced stress on blood cells rather than rely on macroscopic measures of the bulk flow. More sophisticated and accurate calculations may be possible, using numerical simulations. Combined with high-resolution spectral experimental data, these may lead to deeper insight into the mechanisms of flow-induced blood damage, and more reliable design criteria for cardiovascular implants.

6 Conclusions

A simplified mathematical model of the flow of plasma around blood cells has been developed in order to estimate the flow-induced shear stress on suspended cells. Results predict that in laminar flow, the true stress on a cell is approximately equal to the macroscopic shear stress for bulk flow of whole blood. Analysis for turbulent flow, applied to data of Liu et al.[20] for a particular flow through a prosthetic valve, suggest that root mean square true cell stresses are at least an order of magnitude less than the Reynolds stress. These results indicate that the smallest structures in a turbulent flow are not necessarily the most damaging to cells. The analysis suggests that Reynolds stress alone is not adequate as a predictor of cell loading in

turbulent flow. The distribution of energy across length scales is critical to the overall effect of turbulence on blood.

Nomenclature

A, B	functions of f
a	cell radius
E	energy spectral density
f	frequency
K	ratio of stress oscillation amplitude to velocity oscillation amplitude
L	length scale
m	mass
p	pressure
r	radial coordinate
Re	Reynolds number
t	time
u	fluid velocity
$\bar{u}$	mean fluid velocity
u'	fluid velocity fluctuation
v	cell velocity
v'	cell velocity relative to freestream
x_i	Cartesian coordinate
α	phase angle
$\dot{\gamma}$	shear rate
η	Kolmogorov length scale
θ	azimuthal coordinate
μ	dynamic viscosity
ρ	density
σ	stress
ϕ	polar coordinate

Subscripts

0	oscillation amplitude or characteristic scale
c	cell
p	plasma
rms	root mean square
R	Reynolds (stress)
v	viscous (stress)
∞	freestream

Acknowledgements Padraic N. Dooley gratefully acknowledges the support of the Irish Research Council for Science, Engineering and Technology, funded by the National Development Plan.

References

1. Bacher, R. P., Williams, M. C. Hemolysis in capillary flow. *J. Lab. Clin. Med.* 76:485–496, 1970.
2. Bachmann C., Hugo, G., Rosenberg, G., Deutsch, S., Fontaine, A., Tarbell, J.M. Fluid Dynamics of a Pediatric Ventricular Assist Device. Artificial Organs 24:362–372, 2000.
3. Blackshear, P.L. Dorman, F. D., Steinbach, J. H., Maybach, E. J., Singh, A, Collingham, R. E. Shear wall interaction and hemolysis. *Trans. Amer. Soc. Artif. Int. Organs* 12:113–120, 1966.
4. Bradshaw, P. An Introduction to Turbulence and its Measurement. Oxford: Pergamon Press, 1971.
5. Davidson, P. A Turbulence: an introduction for scientists and engineers. Oxford: Oxford University Press, 2004.
6. Day, S. W., McDaniel, J. C., Wood, H. G., Allaire, P. E., Song, X., Lemire, P. P., Miles, S. D. A Prototype HeartQuest Ventricular Assist Device for Particle Image Velocimetry Measurements. *Artif. Organs* 26:1002–1005, 2002.
7. Ellis, J. T., Wick, T. M., Yoganathan, A. P. Prosthesis-induced hemolysis: mechanisms and quantification of shear stress. *J. Heart Valve Dis.*

7:376–386, 1998.

8. Fischer, T. M. The red cell as a fluid droplet: tank tread-Like motion of the human erythrocyte membrane in shear flow. *Science* 202:894–896, 1978.

9. Forstrom, R. J., A new measure of erythrocyte membrane strength: the jet fragility test. Ph.D. Thesis, University of Minnesota, Minneapolis, 1969.

10. Fung, Y. C. Biomechanics: Mechanical Properties of Living Tissues. New York: Springer, 1993.

11. Giersiepen, M., Wurzinger, L. J., Opitz, R., Reul, H. Estimation of shear stress-related blood damage in heart valve prostheses–in vitro comparison of 25 aortic valves. *Int. J Art. Organs* 13:300–306, 1990.

12. Gott, V. L., Alejoa, D. E., Cameron, D. E. Mechanical heart valves: 50 years of evolution. *Ann. Thorac. Surg.* 76:S2230–S2239, 2004.

13. Grigioni, M., Caprari, P., Tarzia, A., D'Avenio, G. Prosthetic heart valves' mechanical loading of red blood cells in patients with hereditary membrane defects. *J. Biomech.* 38:1557–1565, 2005.

14. Hellums, J. D., Brown, C. H. "Blood cell damage by mechanical forces." In: Cardiovascular Flow Dynamics and Measurements. Edited by N.H.C Hwang and N.A Normann. Baltimore: University Park Press 1977.

15. Heuser, G., Opitz, R. A coutte viscometer for short time shearing of blood. *Biorheology* 17:17–24, 1980.

16. Jones, S. A. A relationship between Reynolds stresses and viscous dissipation: implications to red cell damage. *Ann. Biomed. Eng.* 23:21–28, 1995.

17. Kameneva, M. V., Burgreen, G. W., Kono, K., Repko, B., Antaki, J. F., Umezu, M. Effects of turbulent stresses upon mechanical hemolysis: experimental and computational analysis. *Am. Soc. Artif. Intern. Organs J.* 50:418–423, 2004.

18. Landau, L. D., Lifshitz, E. M. Fluid Mechanics, First ed. Oxford: Pergamon Press, 1959.

19. Leverett, L. B., Hellums, J. D., Alfrey, C. P., Lynch, E. C. Red blood cell damage by shear stress. *Biophys. J.* 12:257–273, 1972.

20. Liu, J. S., Lu, P. C., Chu, S. H. Turbulence characteristics downstream of bileaflet aortic valve prostheses. *J. Biomech. Eng.* 122:118–124, 2000.

21. Lu, P. C., Lai, H. C., Liu, J. S. A reevaluation and discussion on the threshold limit for hemolysis in a turbulent shear flow. *J. Biomech.* 34:1361–1364, 2001.

22. Mikeluncak, D. R., Morris, J. F. Stationary shear flow around fixed and free bodies at finite Reynolds number. *J. Fluid Mech.* 520:215–242, 2004.

23. Nevaril, C. G., Lynch, E. C., Alfrey, C. P., Hellums, J. D. Erythrocyte damage and destruction induced by shearing stress. *J. Lab. Clin. Med.* 71:784–790, 1968.

24. Niimi, H., Sugihara, M. Cyclic loading on the red cell membrane in a shear flow: a possible cause of hemolysis. *J. Biomech. Eng.* 107:91–95,

1985.

25. Nobach, H., Müller, E., Tropea, C. Efficient estimation of power spectral density from laser Doppler anemometer data. *Exp. Fluid* 24:499–509, 1998.

26. Paul, R., Apel, J., Klaus, S., Schügner, F., Schwindke, P., Reul, H. Shear stress related blood damage in laminar couette flow. *Artif. Organs* 27:517–529, 2003.

27. Rooney J. A. Hemolysis near an ultrasonically pulsating gas bubble. *Science* 169:869–871, 1970.

28. Sallam, A. M., Hwang, N. H. C., Human red blood cells in a turbulent shear flow: contribution of Reynolds shear stresses. *Biorheology* 21:783–797, 1984.

29. Sutera, S.P., Joist, J. H. "Haematological Effects of Turbulent Blood Flow." In: Thrombosis, Embolism and Bleeding, edited by E.C. Butchart and E. Bodnar. London: ICR Publishers, 1992.

30. Sutera, S. P., Mehrjardi, M. H. Deformation and fragmentation of human red blood cells in turbulent shear flow. *Biophys J* 15:1–10, 1975.

31. Tran-Son-Tay, R., Sutera, S. P., Zahalak, G. I., Rao, P.R. Membrane stress and internal pressure in a red blood cell freely suspended in a shear flow. *Biophys. J.* 51:915–924, 1987.

32. Travis, B. R., Leo, H. L., Shah, P. A., Frakes, D. H., Yoganathan, A. P. An analysis of turbulent shear stresses in leakage flow through a bileaflet mechanical prostheses. *J. Biomech. Eng.* 124:155–165, 2002.

33. Williams, A. R., Hughes, D. E., Nyborg, W. L. Hemolysis near a transversely oscillating wire. *Science* 169:871–873, 1970.

34. Wurzinger, L. J., Opitz, R., Blasberg, P., Schmid-Schoïbein, H. Platelet and coagulation parameters following millisecond exposure to laminar shear stress. *Thromb. Haemost.* 54:381–386, 1985.

35. Wurzinger, L. J., Opitz, R., Eckstein, H. Mechanical bloodtrauma. An overview. *Angéiologie* 38:81–97, 1986.

36. Yin, W., Alemu, Y., Affeld, K., Jesty, J., Bluestein, D. Flow induced platelet activation in bileaflet and monoleaflet mechanical heart valves. *Ann. Biomed. Eng.* 32:1058–1066, 2004.

37. Yoganathan, A. P., He, Z., Casey Jones, S. Fluid mechanics of heart valves. *Annu. Rev. Biomed. Eng.* 6:331–362, 2004.